

Characteristics analysis of rocket projectile based on intelligent morphing technology

XU Yong-jie, WANG Zhi-jun

(College of Mechatronic Engineering, North University of China, Taiyuan 030051, China)

Abstract: Nose deflection control is a new concept of fast response control model. The partial nose of projectile deflects a certain angle relative to the axis of projectile body and then pressure difference emerges on the windward and leeward sides of warhead. Consequently, aerodynamic control force is generated. This control way has high control efficiency and very good application prospects in the ammunition system. Nose deflection actuator based on smart material and structure enables projectile body morphing to obtain additional aerodynamic force and moment, changes the aerodynamic characteristics in the projectile flight process, produces the corresponding balance angle and sideslip angle resulting in motor overload, adjusts flight moving posture to control the ballistics, finally changes shooting range and improves firing accuracy. In order to study characteristics of self-adaptive control projectile, numerical simulations are conducted by using fluid dynamics software ANSYS FLUENT for stabilized rocket projectile. The aerodynamic characteristics at different nose deflection angles, different Mach numbers and different angles of attack are obtained and compared. The results show that the nose deflection control has great influence on the head of rocket projectile, and it causes the asymmetry of the flow field structure and the increase of pressure differences of the warhead on the windward and leeward surface, which results in a larger lift. Finally, ballistics experiments are done for verification. The results can offer theoretical basis for self-adaptive rocket projectile design and optimization and also provide new ideas and methods for field smart ammunition research.

Key words: rocket projectile; intelligent morphing technology; nose deflection; ballistics characteristics

CLD number: TJ415

Document code: A

Article ID: 1674-8042(2015)03-0205-07

doi: 10.3969/j.issn.1674-8042.2015.03.001

0 Introduction

Smartness, intelligence and high mobility of ammunition will be the important development directions of ammunition technology in a long historical period in the future^[1-3]. To research and develop active, detective and self-adaptive ballistic correction and autonomous smart attack ammunition by means of various innovative and intelligent control technologies, simple guidance way or ballistic adaptive way has become the research hotspot of national defense science and technology in the world.

Intelligent morphing technology means that the shape of self-adaptive aircraft changes according to flight mission, flight speed and flight environment.

It uses intelligent material or structure to realize active, adaptive and continuous changes in appearance to meet different missions with different aerodynamic layouts, thus performance optimization of aerodynamic and flight is achieved^[4-7]. For modern high mobility weapons, it can solve the contradictions of different aerodynamic layouts of the aircrafts designed by intelligent morphing technology and improve economic efficiency and operational capability.

Human beings are dedicated to development of lighter and more intelligent missiles now and even for the future. Research on creative and intelligent control technology has very important significance and practical value, where external ballistics plays a key role in this modern missile control technology.

1 Modeling

1.1 Geometrical model

The 3D model of simplified standard fin stabilized rocket projectile is shown in Fig. 1, where length $L=600.0$ mm, and diameter $D=90.0$ mm. The rocket projectile with nose deflection angle δ is shown in Fig. 2.

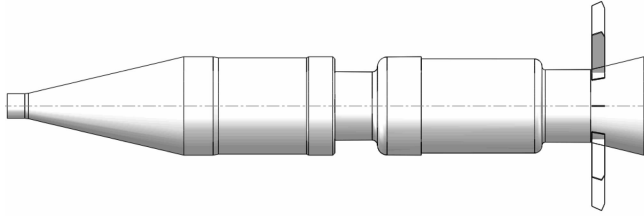


Fig. 1 Standard fin stabilized rocket projectile

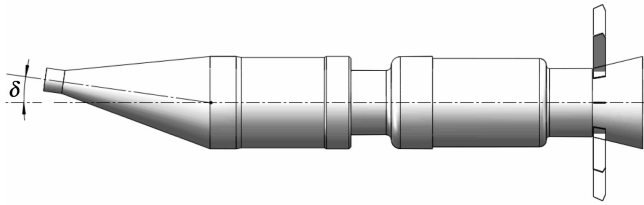


Fig. 2 Rocket projectile with nose deflection angle

1.2 Mass properties

The trajectory correction models for rocket projectiles with different nose deflection angles, including 0° , 2° , 4° , 6° , 8° and 10° , are established. The mass properties of each model are shown in Table 1.

Table 1 Mass properties

Model code	Nose deflection angle $\delta(^{\circ})$	Centroid coordinate (X,Y,Z)		
		X(mm)	Y(mm)	Z(mm)
M ₀	0	331.406	0.000	0.000
M ₁	2	331.889	0.263	0.000
M ₂	4	332.034	0.523	0.001
M ₃	6	332.274	0.778	0.001
M ₄	8	332.608	1.024	0.001
M ₅	10	333.035	1.259	0.002

1.3 Aerodynamic force analysis

According to ballistic theory^[8-9], in the flight process of projectile, regardless of the spinning, in

order to measure the effects from each force and resultant force, all the forces and moments are simplified as the centroid of projectile. For illustrating conveniently, it is shown in Fig. 3.

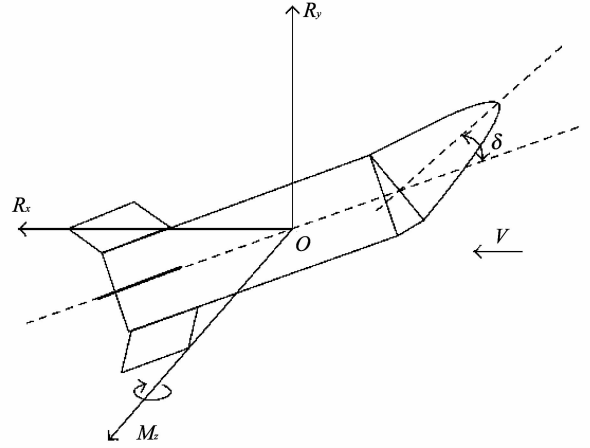


Fig. 3 Diagram for simplifying aerodynamic forces

1) R_x is drag and expressed as

$$R_x = \left(\frac{\rho V^2}{2}\right) S_M C_x,$$

where C_x is drag coefficient and S_M is reference area (m^2).

2) R_y is lift and expressed as

$$R_y = \left(\frac{\rho V^2}{2}\right) S_M C_y,$$

where C_y is drag coefficient and S_M is reference area (m^2).

3) M_z is static moment and expressed as

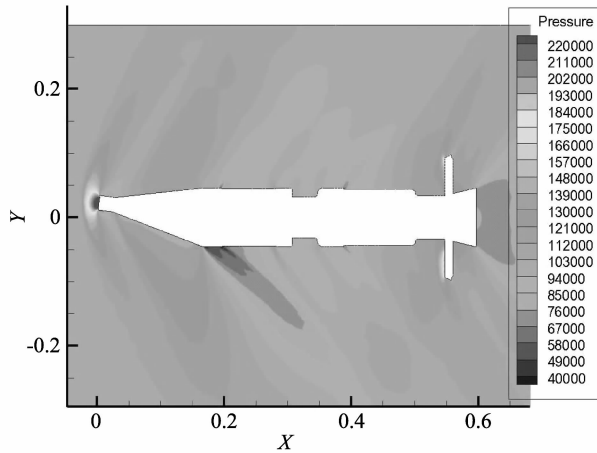
$$M_z = \left(\frac{\rho V^2}{2}\right) S_M m_z,$$

where m_z is moment coefficient.

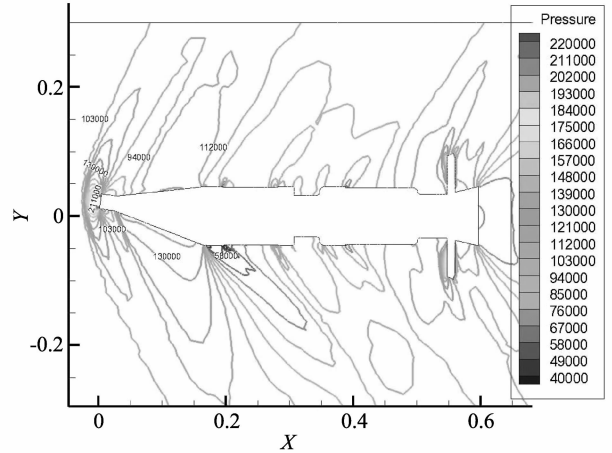
2 Ballistic flight flow field simulation

Mach numbers in simulation are 0.8, 1.0, 1.2, 2.0 and 3.0, respectively, involving subsonic, transonic and supersonic speed ranges; and nose deflection angles contains 0° , 2° , 4° , 6° , 8° and 10° . The dynamics parameters such as flow field velocity and pressure, drag coefficient, lift coefficient and pitching moment coefficient, are obtained by simulation. In computational procedure, single equation model Spalart-Allmaras is used for turbulence model^[10-13],

which only solves a transport equation about the eddy viscosity and obtains good results involving wall limit flow problem and inverse pressure gradient of boundary layer problem. It is commonly used for solving aerodynamic problems of aircraft, flow around airfoil, flow field analysis, and so on.



(a) Pressure nephogram



(b) Pressure contour line

Fig. 4 Pressure field distribution

As shown in Fig. 4, the pressure on projectile increases with the increase of deflection angle. For nose deflection angle of 10° , there is a mutation pressure due to its unsmooth surface. The greater the deflection angle is, the more obvious the mutation pressure is.

The warhead is the most stressful part of the whole projectile, whereby ballistic cap is the most stressful part in the warhead. Its pressure grows with the increase of Mach number and the pressure region has a tendency to gradually expand and gradually move to the rear end of rocket.

When air flows through the pressure region, there is an inflection point of pressure on the shoulder of the rocket, then gas expansion wave emerges. At the same time, a low pressure area emerges in the area near the bottom of the projectile, and it becomes smaller and smaller when Mach number increases, and the speed difference is more and more obvious. The reason is that the rocket empennage impedes the air flow, consequently gas choking phenomenon appears in the empennage leading edge and dilatational wave appears in the empennage trailing edge, finally the interaction leading edge and trailing edge flow

2.1 Pressure field analysis

Typical simulation results of pressure field distribution are shown in Fig. 4. Fig. 4(a) is the pressure nephogram and Fig. 4(b) is the pressure contour line.

field form tail flow field.

In addition, it can be seen that the pressure flow field distribution is asymmetric, and the asymmetry intensifies that because of the existence of nose deflection angle, in front of the shoulder, with the increase of deflection angle, the pressure coefficient on the windward side is larger than that on the leeward side. On the back of the shoulder, with the increase of deflection angle, the pressure coefficient diminishes on the windward side and increases on the leeward side, and the pressure coefficient on the windward side is less than that on the leeward side.

2.2 Velocity field analysis

Typical simulation results of pressure field distribution are shown in Fig. 5. Fig. 5(a) is the pressure nephogram and Fig. 5(b) is the pressure contour line.

As shown in Fig. 5, a high pressure area emerges around warhead in the flight process of external ballistics, and vortex area and stress concentration are around tail.

Deflection angle has important influence on tail flow field. The larger the deflection angle is, the

greater impact it has. Circle flow field changes a lot because of the warhead deflection angle. With the increase of deflection angle, the rocket overall speed

slows down. The head velocity is low, and the low speed region caused by warhead is larger and moves to rear end of the rocket.

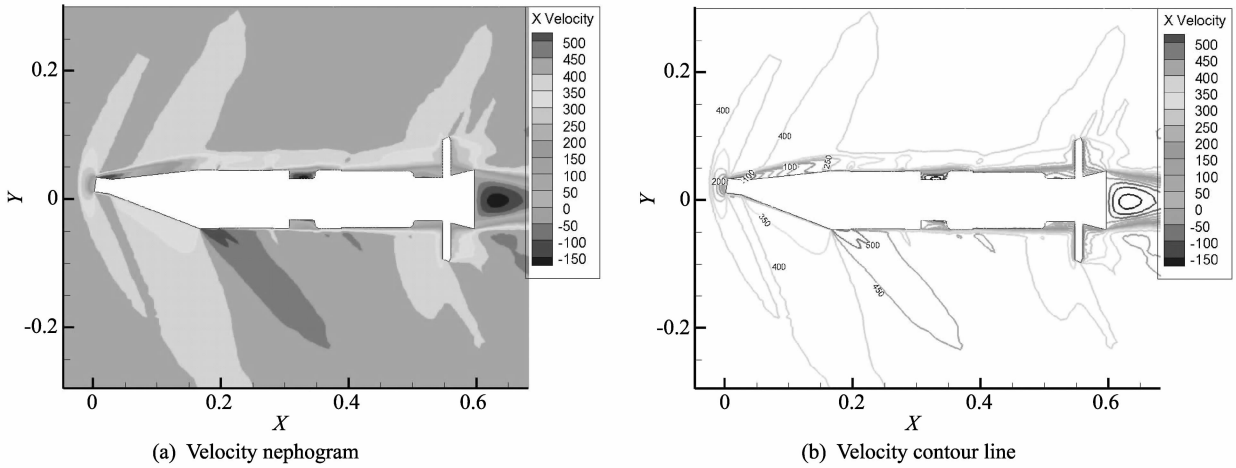


Fig. 5 Velocity field distribution

The larger the deflection angle is, the greater impact it has on the warhead flow field structure and the less impact it has on the downstream flow field. The tail flow field asymmetry increases with the increment of deflection angle. The greater the deflection angle is, the greater warhead disturbance impact it has on the tail flow field. High speed area emerges on the warhead and expansion wave emerges on the shoulder at the same time.

and aerodynamic lift and control torque are limited very much in subsonic velocity range.

There is also a speed-jump on the shoulder windward side because of the existence of attack angle, and the larger Mach number, the larger speed-jump area. The fluid velocity is low in the empennage leading-edge area. Choking phenomenon occurs because of its retardation, and a series of smaller spirals also emerge in the tail flow field due to the speed differences caused by projectile disturbance.

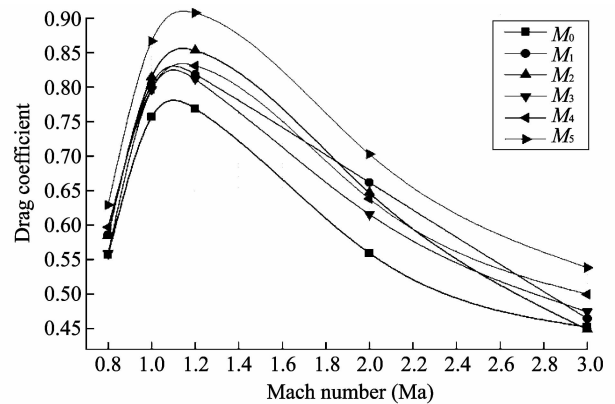


Fig. 6 Drag coefficient when attack angle is 0°

2.3 Aerodynamic characteristics analysis

Calculation of drag coefficient is shown in Fig. 6, and the changing laws of all the models are consistent and the curves change smoothly.

Simulations of lift coefficient and control moment coefficient are shown in Fig. 7.

Under the condition of the same Mach number, when the attack angle is 0°, aerodynamic drag coefficient changes smaller with the change of nose deflection angle. By comparing a large amount of simulation data, rocket projectile's aerodynamic performance is poor in subsonic and transonic velocity ranges

Lift coefficient and additional control torque change obviously when the attack angle is 2° and aerodynamic performance changes significantly. Aerodynamic lift and control moment caused by nose deflection angle are objective and the smaller nose deflection angle can produce large aerodynamic control force.

Control mode of nose deflection can provide greater aerodynamic lift and torque control than rocket projectile without nose deflection angle. Lift coefficient ratio and control moment coefficient ratio of rocket projectile with different nose deflection angles are

shown in Table 2.

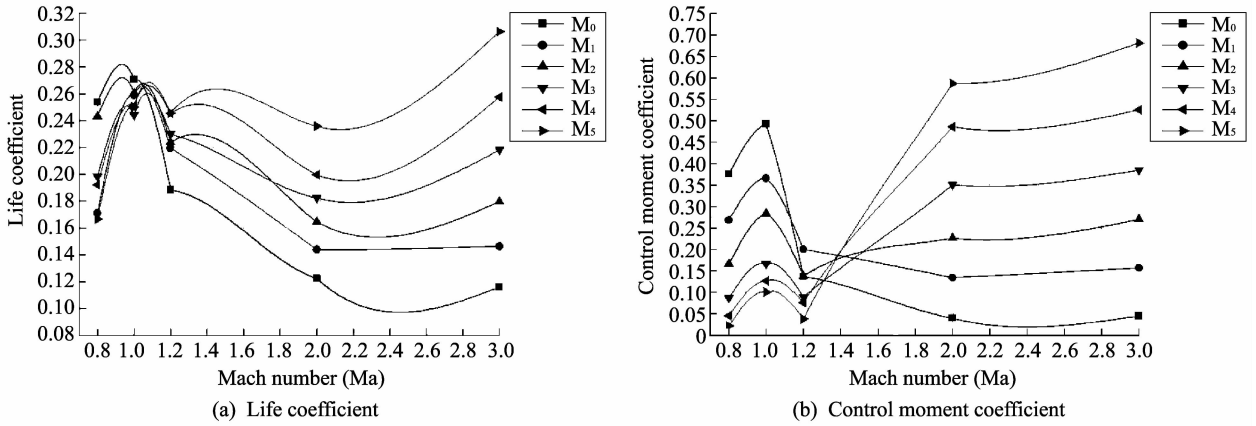


Fig. 7 Aerodynamic coefficient when attack angle is 2°

Table 2 Calculation results of coefficient ratio

Model code	Nose deflection angle $\delta(^{\circ})$	Lift coefficient ratio	Control moment coefficient ratio
M ₁	2	1.26	3.52
M ₂	4	1.55	6.05
M ₃	6	1.88	8.63
M ₄	8	2.22	11.78
M ₅	10	2.64	15.28

In supersonic velocity range, nose deflection angle is 10°. And it can provide the aerodynamic lift 2.64 times and control moment 15.28 times as much as that without nose deflection angle.

3 Experiment

To improve rocket projectile design, the experiments for ballistic correction of rocket projectile with nose deflection angle of 5° was conducted. There are 5 ballistic correction rocket projectiles prepared for the flying experiment^[14-15]. The arrangement for testing is shown in Fig. 8.

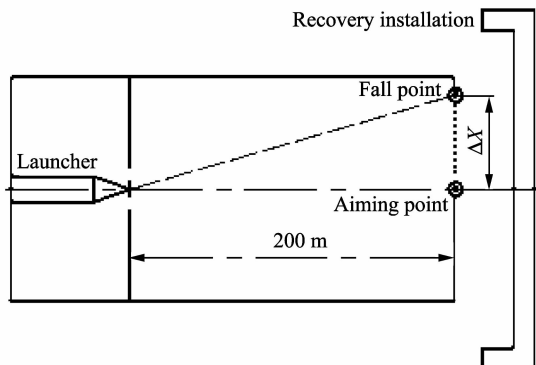


Fig. 8 Arrangement for testing

The distance of 200 m was intercepted in the shooting range direction and the distance between the aiming point and fall point was determined as transverse correction range, marked as ΔX .

In order to get convenient verification, the nose deflection angle was set toward to the same launch direction and the distance between aiming point and fall point was measured as the horizontal correction range caused by nose deflection angle. The experimental results are shown in Table 3. The results show that at the velocity of 151.06 m/s and nose deflection angle being of 5°, the ballistic correction for rocket projectile can obtain horizontal correction range of 0.43 m on the average.

Table 3 Horizontal correction value

Number	Firing range (m)	Correction value $\Delta X(m)$	Flight velocity (m/s)
#1	200	0.44	148.40
#2		0.42	149.80
#3		0.48	152.60
#4		0.39	152.20
#5		0.42	152.30
Average	200	0.43	151.06

4 Conclusions

From the simulation calculation and ballistic experiment on deflectable nose rocket projectile, the following conclusions can be obtained:

1) Large number of aerodynamic simulations show that using nose deflection angle can achieve desired aerodynamic lift, aerodynamic drag and additional

torque control. Furthermore, it can correct ballistic trajectory effectively and realize rocket projectile maneuvering flight.

2) With rocket projectile ballistic correction as fine pneumatic control characteristics in the supersonic velocity range and limited aerodynamic performance in subsonic velocity range. Nose deflection has greater influence on warhead flow field structure and smaller impact on the downstream.

3) With the increase of nose deflection angle, the pressure on the rocket body increases, especially the pressure mutation on the area around the shoulder of the rocket. The flow field changes dramatically and the pressure becomes bigger with the deflection angle being larger. The expansion waves emerge on the shoulder and low pressure area at the bottom of the projectile. The asymmetry of the flow field is bigger and different pressures on the windward and leeward surfaces increase, which result in larger lift.

4) Flight test shows that flying control method of nose deflection is feasible and reliable, thus it can be used for engineering research in the further.

References

- [1] YIN Jian-ping, WANG Zhi-jun. Ammunition theory. Beijing: Beijing Institute of Technology Press, 2014.
- [2] ZHANG Bo, WANG Shu-shan, CAO Meng-yu, et al. Impacts of deflection nose on ballistic trajectory control law. *Mathematical Problems in Engineering*, 2014.
- [3] GAO Ting-xin. Study of aerodynamic characteristics of migraine control. In: *Proceedings of Aviation Aircraft Development and Aerodynamics Seminar*, Hangzhou, 2006.
- [4] ZHANG Tong, ZHAO Xiao-li. Analysis of trajectory correction projectile and its key technology. *Cruise Missile*, 2014, 24(5): 38-42.
- [5] Landers M G, Hall L H, Auman L M, et al. Deflectable nose and canard controls for a fin-stabilized projectile at supersonic and hypersonic speeds. In: *Proceedings of the 21st AIAA Applied Aerodynamics Conference*, Orlando, Florida, 2003; 1.
- [6] XIA Bin, ZHOU Liang. Trajectory correction projectile and analysis on the key technologies for the trajectory correction process. *National Defense Science & Technology*, 2013, 34(3): 27-33.
- [7] Vaughn, M E, Auman L M. Assessment of a productivity-oriented cfd methodology for designing a hypervelocity missile. In: *Proceedings of the 21st AIAA Applied Aerodynamics Conference*, Orlando, Florida, 2003; 23-29.
- [8] HAN Zi-peng. Exterior ballistics of projectile and rockets. Beijing: Beijing Institute of Technology Press, 2014.
- [9] XU Ming-you. Advanced external ballistics. Beijing: Higher Education Press, 2003.
- [10] YU Wen-jie. Study of aerodynamic characteristics for a fin-stabilized projectile with a deflectable nose control. Nanjing: Nanjing University of Science&Technology, 2010.
- [11] WANG Fei, WU Guo-dong, WANG Zhi-jun. Numerical calculation of aerodynamic characteristics of shell with attack angle at the shell head. *Journal of North China Institute of Technology*, 2005, 26(3): 177-179.
- [12] WEI Fang-hai, WANG Zhi-jun, YIN Jian-ping. Numerical calculation of aerodynamic characteristics of shell with an angle of warhead. *Journal of Projectiles, Rockets, Missiles and Guidance*, 2006, 26(1): 553-558.
- [13] DONG Er-bao. Research on realization mechanism and some key technologies of smart morphing aircraft structures. Anhui: University of Science and Technology of China, 2010.
- [14] XU Yu-xin, WANG Shu-shan. Armor-piercing experiment on fragment against sandwich plate with fiber reinforced composite cores. *Acta Materiae Compositae Sinica*, 2012, 29(3): 72-78.
- [15] XU Yu-xin, WANG Shu-shan. Armor-piercing ultimate of tungsten alloy spherical fragment against low-carbon steel. *Journal of Vibration and Shock*, 2011, 30(5): 192-195.

基于智能变形技术的火箭弹特性分析

徐永杰, 王志军

(中北大学 机电工程学院, 山西 太原 030051)

摘要: 偏转头部控制是一种新概念快速响应的控制方式。弹头部相对于弹轴进行局部偏转, 并且在弹头的迎风面和背风面形成压力差从而产生空气控制力, 在弹药系统里, 这是一个高效并具有良好应用前景的控制方式。基于智能材料和结构的弹箭头部智能变形驱动机构可以使弹箭获得额外的控制力和控制力矩, 改变弹丸在飞行过程中的空气动力特性, 在弹箭飞行过程中会产生附加的平衡角、侧滑角, 进而产生机动过载, 控制飞行姿态和飞行弹道, 并在最后时限提高弹丸的射击精确度。为了研究自适应控制弹箭的特性, 利用流体力学软件对尾翼稳定的火箭弹进行了数值模拟。获得不同头部偏角、不同马赫数和不同攻角情况下的弹箭空气动力学特性。结果表明, 偏转头部控制对弹箭的头部具有较大的影响, 并且引起流场的不对称性。弹头部迎风面和背风面的压力差为弹箭提供较大的升力。最后, 做弹道试验验证了仿真的研究结果。研究结果可以为自适应弹箭的设计及优化提供理论基础, 并为智能弹药的研究提供新思路和新方法。

关键词: 火箭弹; 智能变形技术; 头部偏转; 弹道特性

引用格式: XU Yong-jie, WANG Zhi-jun. Characteristics analysis of rocket projectile based on intelligent morphing technology. *Journal of Measurement Science and Instrumentation*, 2015, 6(3): 205-211. [doi: 10.3969/j.issn.1674-8042.2015.03.001]